Regulation of a novel Fusarium cytokinin in Fusarium pseudograminearum

Blum, Ailisa; H. Benfield, Aurelie ; Sørensen, Jens Laurids; Nielsen, Mikkel Rank; Bachleitner, Simone; Studt, Lena; Beccari, Giovanni ; Covarelli, Lorenzo; Batley, Jacqueline; Gardiner, Donald Max

Published in:
Fungal Biology

DOI (link to publication from Publisher):
10.1016/j.funbio.2018.12.009

Publication date:
2019

Document Version
Accepted author manuscript, peer reviewed version

Accepted Manuscript

Regulation of a novel Fusarium cytokinin in Fusarium pseudograminearum

Ailisa Blum, Aurélie H. Benfield, Jens L. Sørensen, Mikkel R. Nielsen, Simone Bachleitner, Lena Studt, Giovanni Beccari, Lorenzo Covarelli, Jacqueline Batley, Donald M. Gardiner

PII: S1878-6146(19)30001-7

DOI: https://doi.org/10.1016/j.funbio.2018.12.009

Reference: FUNBIO 991

To appear in: *Fungal Biology*

Received Date: 9 March 2018

Revised Date: 7 November 2018

Accepted Date: 25 December 2018

Please cite this article as: Blum, A., Benfield, A.H., Sørensen, J.L., Nielsen, M.R., Bachleitner, S., Studt, L., Beccari, G., Covarelli, L., Batley, J., Gardiner, D.M., Regulation of a novel Fusarium cytokinin in Fusarium pseudograminearum, *Fungal Biology*, https://doi.org/10.1016/j.funbio.2018.12.009.

Regulation of a novel Fusarium cytokinin in *Fusarium pseudograminearum*

Ailisa Blum[1,2*], Aurélie H. Benfield[1+], Jens L. Sørensen[3], Mikkel R. Nielsen[3], Simone Bachleitner[4], Lena Studt[4], Giovanni Beccari[5], Lorenzo Covarelli[5#], Jacqueline Batley[2ŧ], Donald M. Gardiner[1,5]

[1]Commonwealth Scientific and Industrial Research Organisation, Agriculture and Food, Queensland Bioscience Precinct, St Lucia, Brisbane, 4067, Australia.

[2]School of Agriculture and Food Science, The University of Queensland, St Lucia, Queensland, 4072, Australia.

[3]Department of Chemistry and Bioscience, Aalborg University, Esbjerg, Denmark, DK-6700.

[4]Department of Applied Genetic and Cell Biology-Tulln, BOKU University of Natural Resources and Life Sciences, Vienna, 3430 Austria.

[5]Department of Agricultural, Food and Environmental Sciences, University of Perugia, Perugia, 06121, Italy.

*Present address: Queensland Brain Institute, The University of Queensland, St Lucia, Queensland, 4072, Australia.

[+]Present address: Institute for Molecular Bioscience, The University of Queensland, St Lucia, Queensland, 4072, Australia.

[ŧ]Present address: School of Biological Sciences, University of Western Australia, Crawley, Western Australia, 6009, Australia.

[#]Present co-address: Centre for Crop and Disease Management, Curtin University, 6102 Bentley, Perth, Australia

Corresponding author: Donald.Gardiner@csiro.au

Abstract

Fusarium pseudograminearum is an agronomically important fungus, which infects many crop plants, including wheat, where it causes Fusarium crown rot. Like many other fungi, the Fusarium genus produces a wide range of secondary metabolites of which only few have been characterized. Recently a novel gene cluster was discovered in *F. pseudograminearum,* which encodes production of cytokinin-like metabolites collectively named Fusarium cytokinins. They are structurally similar to plant cytokinins and can activate cytokinin signalling *in vitro* and *in planta*. Here, the regulation of Fusarium cytokinin production was analysed *in vitro*. This revealed that, similar to deoxynivalenol (DON) production in *F. graminearum*, cytokinin production can be induced *in vitro* by specific nitrogen sources in a pH-dependent manner. DON production was also induced in both *F. graminearum* and *F. pseudograminearum* in cytokinin-inducing conditions. In addition, microscopic analyses of wheat seedlings infected with a *F. pseudograminearum* cytokinin reporter strain showed that the fungus specifically induces its cytokinin production in hyphae, which are in close association with the plant, suggestive of a function of Fusarium cytokinins during infection.

Keywords: cytokinin; wheat; cereal; mycotoxin; GFP; pathogen.

1 Introduction

Fusarium pseudograminearum is a filamentous plant pathogenic fungus, which infects cereal crop plants like wheat and barley, where it can cause both Fusarium crown rot and Fusarium head blight (Obanor et al., 2013). Together Fusarium crown rot and head blight cause up to AU$100 million annual losses to the Australian wheat and barley industry (Murray and Brennan, 2010, 2009). Fusarium crown rot incited by *F. pseudograminearum* is also emerging as a major disease threat in China (Li et al., 2012) and remains a problem in other parts of the world such as Africa and the pacific midwest of the USA (Burgess et al., 2001; HJ et al., 2001; Kazan and Gardiner, 2017; Smiley and Patterson, 1996; van Wyk et al., 1987).

Like other Fusaria, *F. pseudograminearum* produces a wide range of secondary metabolites, for example the mycotoxin deoxynivalenol (DON). In the closely related *F. graminearum,* DON is an important virulence factor during wheat infection and is required for the spread of the fungus from the infection site through the rachis to other florets (Jansen et al., 2005; Proctor et al., 1995). The role of DON in *F. pseudograminearum* during crown rot is not as well understood, but DON seems to be required for the spread of the fungus from the crown and stem base to upper stem nodes (Powell et al., 2017).

Other secondary metabolites produced by *F. pseudograminearum* are the polyketides zearalenone and fusarin and non-ribosomal peptides, like ferricrocin and fusarinine (Hansen et al., 2015). *F. pseudograminearum* also produces the hybrid polyketide-non-ribosomal peptides W493 A and B (Sørensen et al., 2014) which is not found in the closely related species *F. graminearum* and *F. culmorum*. Comparative genome analysis (Hansen et al., 2015) identified 14 putative polyketide synthases (PKS) and 16 non-ribosomal peptide synthases (NRPS) in *F. pseudograminearum*. However, the products of only 8 PKSs and of 4 NPRSs are known (Hansen et al., 2015). Moreover, there are also other classes of secondary metabolites produced by fungi. A genomic analysis of *F. graminearum* identified 67 putative gene clusters with a significant enrichment of predicted secondary metabolism-related enzymatic functions that did not necessarily contain PKS and NRPS genes. Fifty-seven of these had orthologues in *F. pseudograminearum* (Sieber et al., 2014).

Recently a gene cluster, lacking obvious secondary metabolism signature genes such as PKSs or NRPSs, has been identified in *F. pseudograminearum*, which synthesises a novel class of cytokinins, called Fusarium cytokinins (Sørensen et al., 2018). The gene cluster does not exist in the closely related *F. graminearum*, but homologous clusters could be found in *F. oxysporum*, *F. fujikuroi* and *F. verticillioides* (Sørensen et al., 2018).

F. pseudograminearum produces the cytokinins fusatin, fusatinic acid, 8-oxo-fusatin (which are collectively termed Fusarium cytokinins), as well as the more commonly known cytokinins cis-zeatin and trans-zeatin via two different biosynthesis pathways. In the tRNA pathway cis-zeatin is produced via the degradation of prenylated-adenine moieties from tRNA molecules. The Fusarium cytokinins and trans-zeatin are synthesized from adenosine monophosphate and dimethylallyl diphosphate by FCK1 and FCK2, which are encoded in a small cytokinin gene cluster consisting of *FCK1-4*. FCK1 contains two catalytic domains, one is homologous to the catalytic domain of the plant protein LONELY GUY (a cytokinin riboside 5′-monophosphate phosphoribohydrolase) and the other is an isopentyl-transferase and is proposed to be responsible for formation isopentenyladenine (iP) as the initial step of the biosynthetic pathway. In plants these activities are encoded in separate proteins (Kakimoto, 2001; Kurakawa et al., 2007; Takei et al., 2001). FCK2 is a cytochrome P450 monooxygenase proposed to catalyse the downstream steps including hydroxylation and condensation of iP resulting in trans-zeatin and subsequently the Fusarium cytokinins. The function of the other members of the cytokinin gene cluster, FCK3 and FCK4, is still unknown, but their knockouts each resulted in increased production of cytokinins and thus they could be involved in the downstream production of yet unknown compounds. FCK3 contains a putative glycosyl transferase domain and FCK4 a putative alcohol acetyltransferase domain.

The function of the *Fusarium* cytokinins in the pathogenic or saprophytic life stages of *F. pseudograminearum* is still unknown, but the expression of *FCK1*, *FCK2* and *FCK3* is highly induced in *F. pseudograminearum* during barley and *Brachypodium* infection and the *Fusarium* cytokinins accumulate in infected wheat heads in concentration levels similar to those of physiologically active plant cytokinins (Sørensen et al., 2018). In addition, *Fusarium* cytokinins can activate signalling from

an *Arabidopsis* cytokinin receptor in a bacterial reporter strain and fusatinic acid activates cytokinin signalling in *Brachypodium* (Sørensen et al., 2018).

Cytokinins were first identified in plants where they promote cell growth and differentiation, as well as delay leaf senescence (Ferreira and Kieber, 2005). In addition to plants, a vast array of bacteria, algae and fungi are also able to produce cytokinins. During symbiotic mycorrhizal infection of plant roots, cytokinins are produced by both the plant host and the mycorrhizal fungi (Gogala, 1991) and are important for successful colonization and symbiosis, but also to prevent parasitism by the fungus (Cosme et al., 2016; Foo et al., 2013). Similarly, *Rhizobia* root nodule-forming bacteria produce cytokinins to induce the development of symbiotic root nodules in legumes (Phillips and Torrey, 1970). Plant pathogens, such as *Agrobacterium tumefaciens*, also produce cytokinins during plant infection to manipulate their host to their own advantage (Akiyoshi et al., 1984). In addition, locally increased cytokinin levels in plants infected with the biotrophic rust and powdery mildew fungal plant pathogens delay senescence of the infected leaves, which leads to the formation of green islands, though it is not known yet if the fungi produce the cytokinins themselves, or if the host metabolism is altered to induce localized cytokinin production in the plant (Ashby, 2000; Walters et al., 2007). The hemibiotrophic fungus *Pyrenopeziza brassicae* produces cytokinins which might suppress host cell death during brassica infection to allow for the colonization of healthy tissue (Gan and Amasino, 1995; Murphy et al., 1997).

To get a better understanding how Fusarium cytokinin biosynthesis is regulated in *F. pseudograminearum,* different carbon and nitrogen sources as well as different pH were screened. In addition, DON production was also analysed in *F. pseudograminearum* in the different growth conditions. Together the results indicate a similar regulation of DON and Fusarium cytokinin production in *F. pseudograminearum* by specific nitrogen sources in a pH-dependent manner. Further, a Fusarium cytokinin reporter strain was microscopically analysed during wheat seedling infection, which revealed an induction of Fusarium cytokinin production in hyphae in close association with the plant.

2 Materials and Methods

2.1 Fungal strains and wheat cultivar

The wheat cultivar Kennedy was used for the wheat seedling infections. The *F. pseudograminearum* isolate CS3096 was used as wild type strain for wheat seedling infections. The *F. graminearum* DON reporter strain *FgTRI5-GFP* carries a translational C-terminal *GFP* fusion in the endogenous *FgTRI5* locus in the CS3005 *F. graminearum* wild type background (Blum et al., 2016).

2.2 Generation of a cytokinin-GFP reporter strain

The *F. pseudograminearum FpFCK1-GFP* Fusarium cytokinin reporter strain (here after referred to as *FpFCK1-GFP*) carries a C-terminal translational GFP fusion in the endogenous *FpFCK1* locus in the CS3096 *F. pseudograminearum* wild type background. The vector to construct this strain was made using yeast recombinatorial cloning to assemble PCR fragments in pYES2 as previously described (Blum et al., 2016). Cloning details specific to this vector were as follows with primers listed in Table 1. The native promoter and *FCK1* gene were amplified using primers 1-2 from gDNA. A *GFP* fragment (including a four glycine residue linker for the fusion between *FCK1* and *GFP*) was amplified from a previously described TRI5-GFP reporter fusion construct (Blum et al., 2016) using primers 3 and 4. The HSVtk terminator and *gpdA* promoter neomycin phosphotransferase (*nptII*) cassette were amplified from pAN9.1 (Gardiner et al., 2009a) with primers 5-6 and 7-8, respectively. The *FCK1* terminator was amplified from gDNA using primers 9-10. All fragments were amplified using Phusion DNA polymerase (NEB, Ipswich, MA, USA) with annealing temperatures at either 55 or 58°C with 2.5 or 3 minutes extensions in high fidelity buffer as per the manufacturer's instructions. The final construct consisted of, in this order: the native *FCK1* promoter and coding information (including native intron), a four-glycine-linker sequence, *eGFP*, herpes simplex virus thymidine kinase terminator, *Aspergillus nidulans gpdA* promoter, *nptII* and the *FCK1* terminator. The insert of the vector was amplified with primers 11 and 12 which flank the cloning site used in pYES2 for construction (annealing at 53°C using Phusion DNA polymerase), precipitated using 10% polyethylene glycol 8000 (Sigma) and 10 mM $MgCl_2$ (Sigma) and pelleted by centrifugation at 20,000×*g* for 20 minutes in a microcentrifuge. The pellet was washed with 70% ethanol, dried and

resuspended in STC for introduction into *F. pseudograminearum* CS3096 via polyethylene glycol-mediated protoplast transformation as previously described (Desmond et al., 2008).

Transformants were verified by whole genome sequencing and alignment of reads across the *FCK1* locus. Genome sequencing was conducted by the Australian Genome Research Facility (Melbourne, Australia) using Illumina Tru Seq library preparation and sequencing of each isolate in one seventh of an Illumina MiSeq flow cell. Reads were imported into CLCbio genomics workbench, quality trimmed and aligned to the predicted genomic locus to assess for insert copy number and correct integration. These were determined based on manual inspection of read mappings across this region. Raw reads have been deposited in the NCBI sequence read archive under the umbrella bioproject PRJNA389763.

2.3 Fusatin and DON production induction assays

For the induction assays, 10,000 spores were inoculated into 100 µL minimal medium per well in 96 well plates. The minimal medium used was slightly modified from Correll et al., (1987) and contained the following ingredients per litre: 30 g sucrose, 1 g KH_2PO_4, 0.5 g $MgSO_4.7H_2O$, 0.5 g KCl, 10 mg $FeSO_4.7H_2O$, 200 µL of trace element solution (per 100 mL, 5 g citric acid, 5 g $ZnSO_4.7H_2O$, 0.25 g $CuSO_4.5H_2O$, 50 mg $MnSO_4.H_2O$, 50 mg H_3BO_3, 50 mg $NaMoO_4.2H_2O$). Either 40 mM arginine, 40 mM asparagine, 40 mM citrulline, 40 mM citrulline with 5 mM glutamine or just 5 mM glutamine were added as nitrogen sources and the pH adjusted to 4.5 with HCl or pH10 with NaOH. The citrulline medium also contained 0.02 % yeast extract, because the fungus was growing very poorly in the citrulline medium without the yeast extract.

For the inducer screening, 1000 *FpFCK1-GFP* spores were inoculated into 100 µL minimal medium (as above, but with sucrose and nitrogen sources as described below) in PM1, PM3 and PM10 Phenotype MicroArray plates (Biolog, Hayward, USA). In the PM1 plate 5 mM glutamine was added to the minimal medium, in the PM3 plate 90 mM sucrose and in the PM10 plate 5 mM glutamine and 90 mM sucrose.

After inoculation, the 96 well plates were incubated at 28°C in the dark and measured daily with a Perkin Elmer (Waltham, MA, USA) EnVision plate reader fitted

with monochromators. GFP was excited at 488 nm and detected at 509 nm and growth rates were determined by measuring the absorbance at 405 nm (OD_{405}). The GFP intensities were then normalised to the measured biomass as previously described (Blum et al., 2016). Artificially high normalised signals were avoided by only normalising to biomass when biomass was clearly detectable at OD_{405}>0.5 units. Three biological replicates were averaged for each sample. The results from the time course experiment were reproduced three times.

2.4 Fusatin and DON liquid chromatography quantification

The total amounts of fusatin and DON produced after 7 days of growth in 96 well plates were analysed from the same samples which had been analysed for the fusatin and DON production induction assays. For the high performance liquid chromatography (HPLC) quantification the metabolites from the whole fungal colony of each well, as well as the liquid medium, were extracted by adding 100 µL pure methanol and 1000 µL extraction buffer (50% ethyl acetate, 33% methanol, 16% dichloromethane, 1% formic acid) to each sample. Accordingly, the samples were sonicated for ten minutes before they were centrifuged at 20,000×*g* for five minutes. One mL of the supernatant was transferred to a new reaction tube and dried down under a stream of N_2 gas before being resuspended in 50 µL methanol. The samples were centrifuged again at 13,000×*g* for five minutes and 40 µL of the supernatant were transferred into a 300 µL HPLC vial (Phenomenex, Torrance USA). The HPLC system used was a Waters Acquity Arc UHPLC system equipped with a QDa (mass) detector. For the analysis, 5 µL of the samples were injected and separated on a Phenomenex Kinetex phenyl–hexyl column (100 mm × 2.1 mm ID, 2.6 µm) using a flow of 0.4 mL/min with a linear water-acetonitrile gradient, where both eluents were buffered with 0.1% formic acid. The gradient started at 5% acetonitrile and reached 100% in 12 min. Afterwards the solvent conditions were returned to 5% acetonitrile maintained for 8 min to restore starting conditions for the next sample. Single ion monitoring ($[M+H]^+$ ± *m/z* 0.5) with the mass detector run in positive mode and a cone voltage of 10 volts were used for each compound. Three biological replicates were quantified for each treatment.

2.5 Fluorescence microscopy

For the analysis of the subcellular localization of FCK1-GFP, wet mounts of fungal colonies from the 96 well induction assay were analysed with a ZEISS (Oberkochen, Germany) AXIO Imager.M2 with a 100× oil objective. For GFP excitation a 470/40 nm bandpass filter was used and for GFP emission detection a 525/50 nm bandpass filter.

The *FpFCK1-GFP* infected wheat seedlings were analysed with a Leica (Wetzlar, Germany) MZ16 FA fluorescence stereomicroscope with a 1,6× planapochromatic objective. For GFP detection the GFP2 filter set was used with a 425/60 nm excitation filter and a 510 nm longpass filter for emission detection.

2.6 Wheat seedling infection

Wheat seeds cv. Kennedy were sterilized in 10% ethanol with 0.64% sodium hypochlorite for five minutes and washed three times in sterile deionized water. Seven seeds were put onto 150×20 mm petri dishes containing two water soaked filter papers. The plates were wrapped in aluminium foil and placed at 4°C overnight. The next day the plates were transferred to a 20°C plant growth chamber still covered in aluminium foil. After two days, the aluminium foil was removed and the seedlings were infected with 4 µL of either *F. pseudograminearum* wild type *CS3096* spores or *FpFCK1-GFP* spores (10^6 spores per mL). The spores were pipetted either onto the root or the crown of the seedlings. The crown infections were aided by slight puncturing of the plant with the pipette tip.

3 Results

3.1 Construction of a Fusarium cytokinin production reporter strain

A reporter strain was constructed to allow for analysis of the regulation of Fusarium cytokinin production. *GFP* was inserted as a C-terminal translational fusion in the endogenous *FpFCK1* locus in the CS3096 *F. pseudograminearum* wild type background. The whole genomes of four individual transformants were sequenced to allow for selection of correct and single-copy insertion of the construct. Sequence read coverage analysis suggested transformants 221 and 227 were single copy

insertions (Figure 1) and also showed reads consistent with correct insertion at the locus, that is reads all across the key junctions; end of homology flanks, the GFP fusion site and *nptII-FCK1* terminator fusion site (data not shown). In contrast transformant 223 was most likely multi-copy insertion with the homology flanks used in the vector showing increased read coverage (Figure 1). Transformant 224 had lower read coverage, is possibly multicopy and showed reads inconsistent with perfect insertion at the *FpFCK1* locus (data not shown). None of the transformants showed any obvious growth or sporulation defects (data not shown).

3.2 Fusarium cytokinin production can be induced *in vitro* by specific nitrogen sources

Nutrient profiling has previously been applied to identify specific conditions for high level induction of specific secondary metabolites in *F. graminearum* (Gardiner et al., 2009b, 2009c). A similar approach was taken here to identify potential inducers of Fusarium cytokinin production. To this end, the *FpFCK1-GFP* strain was grown in PM1, PM3 and PM10 Phenotype MicroArray plates (Biolog, Hayward, USA). These are commercially available 96-well plates, which contain different carbon sources (PM1), nitrogen sources (PM3) or varying pH (PM10) in each well. None of the carbon sources in the PM1 plate significantly induced FCK1-GFP (data not shown).

Nitrogen source profiling using the PM3 plate revealed asparagine, citrulline, allantoin, and alanine-aspartate and glycine-glutamine dipeptides as weak to moderate inducers of FCK1 expression (Figure 2A). Of these, the alanine-aspartate dipeptide was the strongest inducer (Figure 2A).

In the pH-phenotyping PM10 plate, many growth conditions showed a stronger FCK1-GFP induction (Figure 2B) compared to the PM3 plate (Figure 2A). The strongest FCK1-GFP induction could be observed in the presence of citrulline buffered at pH 4.5 (Figure 2B). Arginine, histidine, threonine and ornithine at pH 4.5 as well as alanine, arginine, isoleucine, proline, ornithine and cadaverine at pH 9.5 also induced FCK1-GFP with intermediate GFP signals (Figure 2B). In contrast to the PM3 plate (Figure 2A), the medium added to the PM10 plate (Figure 2B) also contained 5 mM glutamine and the nitrogen sources in the different wells of the PM10 plate were also at higher concentrations compared to the PM3 plate. These differences, as well as the fact that the medium in the PM10 plates was buffered at a

specific pH, may all contribute to the stronger FCK1-GFP induction observed in the PM10 plate (Figure 2B).

Since the exact contents of the phenotype microarray plates is proprietary information, validation of the identified inducing conditions was undertaken. In PM3 plates the nitrogen sources are expected to be around 5 mM. In the PM10 plates the nitrogen sources are at approximately 40 mM, an undisclosed buffer at 60 mM and yeast extract (0.02%) is also present (Biolog, personal communication). The validation was undertaken using time course experiments with the *FpFCK1-GFP* reporter strain. Standard 96-well plates with minimal media, which only contained one specific nitrogen source were used, rather than the two which were present in the PM10 profiling plates. The fungus was grown in media containing arginine, asparagine or citrulline at 40 mM and the pH was adjusted to either pH 4.5 or pH 10 with hydrogen chloride and sodium hydroxide, respectively. Asparagine was chosen, because it was able to induce FCK1-GFP without the presence of an additional nitrogen source in the PM3 plates and in combination with alanine resulted in the strongest FCK1-GFP induction on the PM3 plate (Figure 2A). Citrulline was also included in this experiment, because it showed the strongest FCK1-GFP induction on the PM10 plate and some induction in PM3 (Figure 2). In addition, FCK1-GFP induction was also analysed in arginine, as arginine has been reported before as an inducer of DON production in the closely related *F. graminearum*.

After three days, both asparagine and arginine induced FCK1-GFP, with the strongest induction observed in arginine (Figure 3A). FCK1-GFP induction by arginine and asparagine was pH-dependent and could be suppressed by a high pH (Figure 3A). No significant FCK1-GFP signals could be detected in citrulline during the seven-day time course (Figure 3A).

As the media in the PM10 plate (Figure 2B) also contained 5 mM glutamine, the FCK1-GFP induction assay was repeated with 40 mM citrulline with 5 mM glutamine added. In combination with glutamine, citrulline induced FCK1-GFP after four days, though to a lesser extent than arginine and asparagine (Figure 3B). Similar to arginine and asparagine, the induction by citrulline and glutamine was also pH dependent (Figure 3B). The induction seems to be specific to citrulline, as no significant FCK1-GFP induction could be detected in 5 mM glutamine until day seven (Figure 3B).

3.3 Fusatin production is reminiscent of DON production in different growth conditions in axenic culture in *F. pseudograminearum*

It had been shown previously for a *F. graminearum FgTRI5-GFP* DON reporter strain, that the TRI5-GFP expression levels reflect the levels of DON produced by the fungus (Blum et al., 2016). However, expression levels of biosynthesis enzymes may not necessarily reflect the production levels of a compound. Thus, it is not known if the FCK1-GFP expression levels correlate to the fusatin production levels. Accordingly, the total fusatin levels produced by the *FpFCK1-GFP* reporter strain during the previous time course experiment (Figure 3) were quantified by high performance liquid chromatography (HPLC) coupled to a mass spectrometer. In addition, the total DON levels were quantified in the same samples. As arginine is known to induce TRI5-GFP expression in *F. graminearum* (Blum et al., 2016; Gardiner et al., 2009b), we wanted to know if *F. pseudograminearum* was also producing DON when fusatin biosynthesis was induced.

Overall, the *FpFCK1-GFP* reporter strain produced 10-50-fold less fusatin than the CS3096 wild type strain and 2-40-fold more DON than CS3096 (Figure 4). However, these differences in production levels (i.e. decreased fusatin and increased DON in the reporter strain compared to the parent) were not statistically significant, with the exception of DON production in citrulline and asparagine at pH 4.5 (Figure 4B). The lack of significance means that the reporter strain behaviour is reflective of the parental strain with respect to these secondary metabolites. The *FpFCK1-GFP* and CS3096 showed similar responses of fusatin and DON production in the different growth conditions (Figure 4) and the fusatin levels reflect the FCK1-GFP expression patterns (Figure 3). As an exception, high fusatin levels could be detected in citrulline in both the *FpFCK1-GFP* reporter strain and the CS3096 wild type (Figure 4 A), whereas no significant FCK1-GFP signals were detected in citrulline (Figure 3 A). Generally, the fusatin levels were about 100-1000-fold lower than the DON levels (on a weight for weight basis), however it is known, that plant cytokinins and other phytohormones are active at very low concentrations. DON and fusatin production in *F. pseudograminearum* were pH dependent, as high pH suppressed or reduced DON and fusatin production in otherwise inductive nitrogen sources (Figure 4). This is in accordance with previous results showing the acid pH dependence of DON production in *F. graminearum* (Gardiner et al., 2009c; Merhej et al., 2011) as well as

the pH dependence of the FCK1-GFP expression levels (Figure 3). The only exception was a non-significant increase in DON production in CS3096 in asparagine in pH 10 in comparison to pH 4.5. Only one of the three replicates produced detectable amounts of DON at pH10.

In summary, the *FpFCK1-GFP* reporter strain is a useful tool to identify conditions of high fusatin production, but the FCK1-GFP levels do not perfectly correlate with the levels of fusatin. In addition, the GFP tag in the *FpFCK1-GFP* reporter strain seems to decrease the efficiency of fusatin production, which in turn seems to indirectly increase DON production.

3.4 The fusatin biosynthesis enzyme FCK1 is localized in the cytosol

As the *FpFCK1-GFP* reporter strain carries a translational GFP fusion, the subcellular localization of FCK1-GFP was analysed by fluorescence microscopy. Similar to the DON biosynthesis enzyme TRI5 in *F. graminearum* (Blum et al., 2016; Boenisch et al., 2017), the *F. pseudograminearum* FCK1-GFP is also localized in the cytosol (Figure 5). Under the fusatin biosynthesis-inducing conditions, *F. pseudograminearum* also developed ovoid cells (Figure 5, second row), which are similar to those previously observed in *F. graminearum* during DON biosynthesis-inducing conditions (Blum et al., 2016; Menke et al., 2013).

3.5 *F. pseudograminearum* specifically induces fusatin biosynthesis during infection in hyphae in close contact with the plant

To get a better understanding of whether fusatin is involved in plant infection by *F. pseudograminearum*, wheat seedlings were infected with the *FpFCK1-GFP* reporter strain and analysed by fluorescence microscopy. During the course of infection, there was substantial hyphal growth on the outside of the infected seedlings, yet no FCK1-GFP signals could be detected in the hyphae growing on the seedling surface (Figure 6A,B). When the infection was repeated, very weak GFP signals could be seen in some hyphae above the crown and the start of the roots, as well as in some hyphae growing out of the top of the coleoptile (not shown). However, when the coleoptile was pulled back 10 days after infection, clear GFP signals could be detected in densely packed hyphae on the inside of the coleoptile as well as on the pseudostem, which was previously covered in the coleoptile (Figure 6C,D). In addition, after removal of the coleoptile the outer leaf was sliced

open to reveal the younger leaf. Between the two leaves many fluorescing hyphae could be detected which were interconnected by hyphal clumps (Figure 6E,F). The FCK1-GFP signal intensities were much higher in the hyphae growing in between the leaves and the coleoptile than the signal intensities in hyphae growing on the surface, so that no signals could be detected in the hyphae on the surface with the acquisition settings used for the hyphae in between leaves.

Fifteen days after infection the coleoptile was almost fully dried out and no fluorescing hyphae could be found underneath (not shown). However, when the leaves were pulled apart, strong FCK1-GFP signals could be detected in dense hyphal mats, which were in close association with the inside of the first leaf (Figure 7A,B). When the second leaf was removed, the surface of the third and youngest leaf was revealed to be intensely colonised by the fungus and most hyphae showed GFP signals (Figure 7C,D). The weak signals of the roots (Figure 7A,B, first column) appeared to be autofluorescence of the roots. Similarly, the signals which can be seen from the dead coleoptile as well as some parts of the first and second leaves in column one of C and D of Figure 7, are due to autofluorescence of dead tissue.

The infections were repeated with an independent spore preparation, which also included another *FpFCK1-GFP* transformant. This experiment showed that the above- described scenarios were not specific to a certain time point after infection, but rather seemed to be dependent on the course of infection in each individual plant. Fluorescing hyphae in between the coleoptile and the pseudostem were usually found during earlier infection stages, when the crown was already brown, but the leaves did not show symptoms yet. The fluorescing hyphae in the pseudostem in between the leaves were found when the infection had progressed further and the leaves were showing clear symptoms. However, during final infection stages, when the plant tissue was completely necrotic, none of the hyphae within the plant were fluorescing. Thus, FCK1-GFP seems to be mainly induced in hyphae growing in close association with the plant in between living plant tissue, and less in dead tissue or outside the plant.

Wheat seedlings were also infected with the CS3096 *F. pseudograminearum* wild type strain (Figure 7E,F). A similar auto fluorescence could be observed from dead plant tissue, which can be seen in the background in Figure 7F, but as expected no fluorescence could be detected in the hyphae.

4 Discussion

Here we show that the expression of the *F. pseudograminearum* fusatin biosynthesis enzyme FCK1 can be induced *in vitro* by specific nitrogen sources, similar to the DON biosynthesis enzyme TRI5 in *F. graminearum* (Gardiner et al., 2009b). During the seven-day time course experiment high concentrations of asparagine, arginine and citrulline in combination with glutamine induced FCK1-GFP in *F. pseudograminearum*. FCK1-GFP was only induced in low pH and high pH repressed otherwise inducing conditions. This is similar to TRI5-GFP expression during DON production in *F. graminearum*, which is also dependent on low pH (Gardiner et al., 2009c). The DON levels produced by the *F. pseudograminearum FpFCK1-GFP* strain showed similar patterns to the fusatin levels in the different nitrogen sources and the production of both was pH dependent. Thus, fusatin and DON production seem to share similar regulatory mechanisms in *F. pseudograminearum*.

In comparison to the CS3096 wild type *F. pseudograminearum*, the *FpFCK1-GFP* reporter strain produced less fusatin and more DON. The decrease in fusatin production is most likely due to the GFP tag, as this was inserted in the endogenous *FpFCK1* locus as a translational fusion. The increase in DON production could be caused by a shift in a precursor pool, as fusatin and DON are synthesized from dimethylallyl pyrophosphate and farnesyl pyrophosphate respectively, which are both produced via the mevalonate pathway. Thus, the decreased fusatin production might indirectly cause an increase in precursor availability for DON production.

Similar to DON production in *F. graminearum*, *F. pseudograminearum* develops ovoid cells in asparagine containing medium, however as the fungus also produces DON under these conditions, the cellular development could also be linked to DON production. Nevertheless, in *F. pseudograminearum* FCK1-GFP is expressed in these ovoid cells and is localised in the cytosol, similar to TRI5-GFP in *F. graminearum* (Blum et al., 2016; Boenisch et al., 2017).

Although, previous experiments indicated that fusatin behaves as a cytokinin and that it can induce cytokinin signalling in *Brachypodium* (Sørensen et al., 2018), the actual function of fusatin in *F. pseudograminearum* is still unknown. Our previous work described that (as data not shown) the FCK1 mutant strain did not alter

infectivity (Sørensen et al., 2018), although analyses of these mutants is complicated by the presence of the tRNA-derived cytokinin pathway in *F. pseudograminearum*. Using *F. graminearum* strains carrying the Fusarium cytokinin cluster (Sørensen et al., 2018) a trend towards reductions in FHB and seedling disease severity, and reduced chlorosis in the FHB assays, was observed although this was only statistically significant for one transformant (Supplementary Figure 1). The microscopic analysis of *FpFCK1-GFP* infected wheat seedlings also indicates that fusatin might play a role during wheat infection, as FCK1-GFP is mainly induced in hyphae growing in close association with living plant tissue. However, not all hyphae growing in between leaves were fluorescing. This seemed to be most often the case, when the plant tissue showed substantial cell death, but also when there was no cell death at all. Often, FCK1-GFP positive hyphae could be found in a zone in between mainly dead tissue and the still healthy tissue, where cell death was starting to occur in some isolated cell groups. Thus, fusatin might play a role during a very specific time point of infection, which seems to be in between the biotrophic and the necrotrophic phase of infection. Although *in vitro* fusatin production-inducing conditions also induce DON production, this does not necessarily mean that they would be coproduced during the same infection stages or in the same hyphae at the same time. It would be interesting to introduce a DON reporter construct, like TRI5-RFP, into the *FpFCK1-GFP* strain to analyse the spatial and temporal production of these two secondary metabolites during plant infection at the same time.

In other plant pathogenic fungi cytokinins are produced during plant infection to delay senescence and to allow the colonization of healthy plant tissue by the fungus (Ashby, 2000; Gan and Amasino, 1995; Murphy et al., 1997; Walters and McRoberts, 2006). Accordingly, fusatin could play a similar role in *F. pseudograminearum* during wheat infection and suppress host cell death to allow the spread of the fungus in the still healthy plant tissue before the fungus switches to the necrotrophic infection phase during which DON production is potentially induced to kill the plant cells. The trends observed with the infection assays with the *F. graminearum* strains expressing cytokinins are consistent with this hypothesis, although further testing with additional genetic material such as a *F. pseudograminearum* double mutant lacking both cytokinin pathways is required. In addition to delaying senescence, plant cytokinins also increase the sink strength,

especially in younger plant tissue (Leopold and Kawase, 1964; Richmond and Lang, 1957; Roitsch and Ehneß, 2000). Hence, *F. pseudograminearum* could produce fusatin to manipulate the tissue it is infecting to become a sink tissue, so there will be more nutrients available for the fungus. On the other hand, cytokinins have also been shown to regulate the accumulation of defense metabolites in different plant species (Brütting et al., 2017; Dervinis et al., 2010; Schäfer et al., 2015; Smigocki et al., 1993) which would be counterproductive for the fungus during infection. Thus, it would be very interesting to see if the Fusarium cytokinins are able to only activate certain cytokinin signalling pathways in the plant which are beneficial for the fungus, but are able to avoid those that would induce plant defense responses. However, the cost of the plant defense metabolite accumulation, might also be less than the benefit of the nutrient accumulation for the fungus. In addition, *F. pseudograminearum* is able to detoxify wheat benzoxazolinone defense metabolites (Kettle et al., 2015) and thus may have evolved to tolerate the accumulation of certain plant defense metabolites. In summary, the data so far support a potential role of the *F. pseudograminearum* produced cytokinins during wheat infection, however the exact mechanisms of action still remain to be revealed.

5 Acknowledgements

AB was supported by a University of Queensland Graduate Research Scholarship and the Australian Grains Industry Research and Development Corporation's Grains Research Scholarship (GRS10658) fellowship. SB and LS were supported by the Austrian Science Fund (FWF) projects F-3703 and M 2149-B22. Part of this work was undertaken in the Department of Agricultureal, Food and Environmental Sciences of the University of Perugia, Italy, as part of an Endeavour Executive Fellowship awarded to DMG by the Australian Government.

6 References

Akiyoshi, D.E., Klee, H., Amasino, R.M., Nester, E.W., Gordon, M.P., 1984. T-DNA of *Agrobacterium tumefaciens* encodes an enzyme of cytokinin biosynthesis. Proc. Natl. Acad. Sci. 81, 5994–5998. https://doi.org/10.1073/pnas.81.19.5994

Ashby, A.M., 2000. Biotrophy and the cytokinin conundrum. Physiol. Mol. Plant Pathol. 57, 147–158. https://doi.org/10.1006/pmpp.2000.0294

Blum, A., Benfield, A.H., Stiller, J., Kazan, K., Batley, J., Gardiner, D.M., 2016. High-throughput FACS-based mutant screen identifies a gain-of-function allele of the *Fusarium graminearum* adenylyl cyclase causing deoxynivalenol over-production. Fungal Genet. Biol. 90, 1–11. https://doi.org/10.1016/j.fgb.2016.02.005

Boenisch, M.J., Broz, K.L., Purvine, S.O., Chrisler, W.B., Nicora, C.D., Connolly, L.R., Freitag, M., Baker, S.E., Kistler, H.C., 2017. Structural reorganization of the fungal endoplasmic reticulum upon induction of mycotoxin biosynthesis. Sci. Rep. 7, 44296. https://doi.org/10.1038/srep44296

Brütting, C., Schäfer, M., Vanková, R., Gase, K., Baldwin, I.T., Meldau, S., 2017. Changes in cytokinins are sufficient to alter developmental patterns of defense metabolites in Nicotiana attenuata. Plant J. 89, 15–30. https://doi.org/10.1111/tpj.13316

Burgess, L.W., Backhouse, D., Summerell, B.A., Swan, L.J., 2001. Crown rot of wheat, in: Summerell, B., Leslie, J., Backhouse, D., Bryden, W., Burgess, L. (Eds.), Fusarium: Paul E. Nelson Memorial Symposium. APS Press, St Paul, MN, USA, pp. 271–294.

Correll, J.C., Klittich, C.J.R., Leslie, J.F., 1987. Nitrate nonutilizing mutants of *Fusarium oxysporum* and their use in vegetative compatibility tests. Phytopathology 77, 1640–1646.

Cosme, M., Ramireddy, E., Franken, P., Schmülling, T., Wurst, S., 2016. Shoot- and root-borne cytokinin influences arbuscular mycorrhizal symbiosis. Mycorrhiza 26, 709–720. https://doi.org/10.1007/s00572-016-0706-3

Dervinis, C., Frost, C.J., Lawrence, S.D., Novak, N.G., Davis, J.M., 2010. Cytokinin primes plant responses to wounding and reduces insect performance. J. Plant Growth Regul. 29, 289–296. https://doi.org/10.1007/s00344-009-9135-2

Desmond, O.J., Manners, J.M., Stephens, A.E., Maclean, D.J., Schenk, P.M., Gardiner, D.M., Munn, A.L., Kazan, K., 2008. The *Fusarium* mycotoxin deoxynivalenol elicits hydrogen peroxide production, programmed cell death and defence responses in wheat. Mol. Plant Pathol. 9, 435–445. https://doi.org/10.1111/j.1364-3703.2008.00475.x

Ferreira, F.J., Kieber, J.J., 2005. Cytokinin signaling. Curr. Opin. Plant Biol. 8, 518–525. https://doi.org/10.1016/j.pbi.2005.07.013

Foo, E., Ross, J.J., Jones, W.T., Reid, J.B., 2013. Plant hormones in arbuscular mycorrhizal symbioses: an emerging role for gibberellins. Ann. Bot. 111, 769–779. https://doi.org/10.1093/aob/mct041

Gan, S., Amasino, R.M., 1995. Inhibition of leaf senescence by autoregulated production of cytokinin. Science (80-.). 270.

Gardiner, D.M., Kazan, K., Manners, J.M., 2009a. Novel genes of *Fusarium graminearum* that negatively regulate deoxynivalenol production and virulence. Mol. Plant. Microbe. Interact. 22, 1588–1600. https://doi.org/10.1094/MPMI-22-12-1588

Gardiner, D.M., Kazan, K., Manners, J.M., 2009b. Nutrient profiling reveals potent inducers of trichothecene biosynthesis in *Fusarium graminearum*. Fungal Genet. Biol. 46, 604–613. https://doi.org/10.1016/j.fgb.2009.04.004

Gardiner, D.M., Osborne, S., Kazan, K., Manners, J.M., 2009c. Low pH regulates the production of deoxynivalenol by *Fusarium graminearum*. Microbiology 155, 3149–3156. https://doi.org/10.1099/mic.0.029546-0

Gogala, N., 1991. Regulation of mycorrhizal infection by hormonal factors produced by hosts and fungi. Experientia 47, 331–340. https://doi.org/10.1007/BF01972074

Hansen, F.T., Gardiner, D.M., Lysøe, E., Fuertes, P.R., Tudzynski, B., Wiemann, P., Sondergaard, T.E., Giese, H., Brodersen, D.E., Sørensen, J.L., 2015. An update to polyketide synthase and non-ribosomal synthetase genes and nomenclature in *Fusarium*. Fungal Genet. Biol. 75, 20–29. https://doi.org/10.1016/j.fgb.2014.12.004

HJ, B., Mergoum, M., Morgounov, A., Nicol, J., 2001. Adaptation of winter wheat to central and west Asia. CIMMYT research results. CIMMYT.

Jansen, C., von Wettstein, D., Schäfer, W., Kogel, K.-H., Felk, A., Maier, F.J., 2005. Infection patterns in barley and wheat spikes inoculated with wild-type and trichodiene synthase gene disrupted *Fusarium graminearum*. Proc. Natl. Acad. Sci. U. S. A. 102, 16892–16897. https://doi.org/10.1073/pnas.0508467102

Kakimoto, T., 2001. Identification of plant cytokinin biosynthetic enzymes as dimethylallyl diphosphate:ATP/ADP isopentenyltransferases. Plant Cell Physiol. 42, 677–685. https://doi.org/10.1093/pcp/pce112

Kazan, K., Gardiner, D., 2017. Fusarium crown rot caused by Fusarium pseudograminearum in cereal crops: recent progress and future prospects. Mol. Plant Pathol. In press. https://doi.org/10.1111/mpp.12639

Kettle, A.J., Batley, J., Benfield, A.H., Manners, J.M., Kazan, K., Gardiner, D.M., 2015. Degradation of the benzoxazolinone class of phytoalexins is important for virulence of Fusarium pseudograminearum towards wheat. Mol. Plant Pathol. 16, 946–962. https://doi.org/10.1111/mpp.12250

Kurakawa, T., Ueda, N., Maekawa, M., Kobayashi, K., Kojima, M., Nagato, Y., Sakakibara, H., Kyozuka, J., 2007. Direct control of shoot meristem activity by a cytokinin-activating enzyme. Nature 445, 652–655. https://doi.org/10.1038/nature05504

Leopold, A.C., Kawase, M., 1964. Benzyladenine effects on bean leaf growth and senescence. Am. J. Bot. 51, 294. https://doi.org/10.2307/2440299

Li, H.L., Yuan, H.X., Fu, B., Xing, X.P., Sun, B.J., Tang, W.H., 2012. First report of *Fusarium pseudograminearum* causing crown rot of wheat in Henan, China. Plant Dis. 96, 1065. https://doi.org/10.1094/PDIS-01-12-0007-PDN

Menke, J., Weber, J., Broz, K., Kistler, H.C., 2013. Cellular development associated with induced mycotoxin synthesis in the filamentous fungus *Fusarium graminearum*. PLoS One 8, e63077. https://doi.org/10.1371/journal.pone.0063077

Merhej, J., Richard-Forget, F., Barreau, C., 2011. The pH regulatory factor Pac1 regulates Tri gene expression and trichothecene production in Fusarium graminearum. Fungal Genet. Biol. https://doi.org/10.4324/9781315309217

Murphy, A.M., Pryce-Jones, E., Johnstone, K., Ashby, A.M., 1997. Comparison of cytokinin production *in vitro* by *Pyrenopeziza brassicae* with other plant pathogens. Physiol. Mol. Plant Pathol. 50, 53–65. https://doi.org/10.1006/pmpp.1996.0070

Murray, G.M., Brennan, J.P., 2010. Estimating disease losses to the Australian

barley industry. Australas. Plant Pathol. 39, 85–96. https://doi.org/10.1071/AP09064

Murray, G.M., Brennan, J.P., 2009. Estimating disease losses to the Australian wheat industry. Australas. Plant Pathol. 38, 558–570. https://doi.org/10.1071/AP09053

Obanor, F., Neate, S., Simpfendorfer, S., Sabburg, R., Wilson, P., Chakraborty, S., 2013. *Fusarium graminearum* and *Fusarium pseudograminearum* caused the 2010 head blight epidemics in Australia. Plant Pathol. 62, 79–91. https://doi.org/10.1111/j.1365-3059.2012.02615.x

Phillips, D.A., Torrey, J.G., 1970. Cytokinin production by *Rhizobium japonicum*. Physiol. Plant. 23, 1057–1063. https://doi.org/10.1111/j.1399-3054.1970.tb08880.x

Powell, J.J., Carere, J., Fitzgerald, T.L., Stiller, J., Covarelli, L., Xu, Q., Gubler, F., Colgrave, M.L., Gardiner, D.M., Manners, J.M., Henry, R.J., 2017. The Fusarium crown rot pathogen *Fusarium pseudograminearum* triggers a suite of transcriptional and metabolic changes in bread wheat (*Triticum aestivum L.*). Ann. Bot. 119, 853–867. https://doi.org/10.1093/aob/mcw207

Proctor, R.H., Hohn, T.M., McCormick, S.P., 1995. Reduced virulence of *Giberella zeae* caused by disruption of a trichothecene toxin biosynthetic gene. Mol. Plant. Microbe. Interact. 8, 593–601.

Richmond, A.E., Lang, A., 1957. Effect of kinetin on protein content and survival of detached Xanthium Leaves. Science (80-.). 125, 650–651.

Roitsch, T., Ehneß, R., 2000. Regulation of source/sink relations by cytokinins. Plant Growth Regul. 32, 359–367. https://doi.org/10.1023/A:1010781500705

Schäfer, M., Meza-Canales, I.D., Brütting, C., Baldwin, I.T., Meldau, S., 2015. Cytokinin concentrations and CHASE-DOMAIN CONTAINING HIS KINASE 2 (NaCHK2)- and NaCHK3-mediated perception modulate herbivory-induced defense signaling and defenses in *Nicotiana attenuata*. New Phytol. 207, 645–658. https://doi.org/10.1111/nph.13404

Sieber, C.M.K., Lee, W., Wong, P., Münsterkötter, M., Mewes, H.-W., Schmeitzl, C., Varga, E., Berthiller, F., Adam, G., Güldener, U., 2014. The *Fusarium*

graminearum genome reveals more secondary metabolite gene clusters and hints of horizontal gene transfer. PLoS One 9, e110311. https://doi.org/10.1371/journal.pone.0110311

Smigocki, A., Neal, J.W., McCanna, I., Douglass, L., 1993. Cytokinin-mediated insect resistance in *Nicotiana* plants transformed with the ipt gene. Plant Mol. Biol. 23, 325–335. https://doi.org/10.1007/BF00029008

Smiley, R.W., Patterson, L.-M., 1996. Pathogenic fungi associated with *Fusarium* foot rot of winter wheat in the semiarid Pacific Northwest. Plant Dis. 80, 944–949.

Sørensen, J.L., Benfield, A.H., Wollenberg, R.D., Westphal, K., Wimmer, R., Nielsen, M.R., Nielsen, K.F., Carere, J., Covarelli, L., Beccari, G., Powell, J., Yamashino, T., Kogler, H., Sondergaard, T.E., Gardiner, D.M., 2018. The cereal pathogen Fusarium pseudograminearum produces a new class of active cytokinins during infection. Mol. Plant Pathol. https://doi.org/10.1111/mpp.12593

Sørensen, J.L., Sondergaard, T.E., Covarelli, L., Fuertes, P.R., Hansen, F.T., Frandsen, R.J.N., Saei, W., Lukassen, M.B., Wimmer, R., Nielsen, K.F., Gardiner, D.M., Giese, H., 2014. Identification of the biosynthetic gene clusters for the lipopeptides Fusaristatin A and W493 B in Fusarium graminearum and F. pseudograminearum. J. Nat. Prod. 77, 2619–2625. https://doi.org/10.1021/np500436r

Takei, K., Sakakibara, H., Sugiyama, T., 2001. Identification of genes encoding adenylate isopentenyltransferase, a cytokinin biosynthesis enzyme, in Arabidopsis thaliana. J. Biol. Chem. 276, 26405–26410. https://doi.org/10.1074/jbc.M102130200

van Wyk, P.S., Los, O., Pauer, G.D.C., Marasas, W.F.O., 1987. Geographic distribution and pathogenecity of *Fusarium* species associated with crown rot of wheat in the Orange Free State, South Africa. Phytophylactica 19, 271–274.

Walters, D.R., McRoberts, N., 2006. Plants and biotrophs: a pivotal role for cytokinins? Trends Plant Sci. 11, 581–586. https://doi.org/10.1016/j.tplants.2006.10.003

Walters, D.R., McRoberts, N., Fitt, B.D.L., 2007. Are green islands red herrings?

Significance of green islands in plant interactions with pathogens and pests. Biol. Rev. 83, 79–102. https://doi.org/10.1111/j.1469-185X.2007.00033.x

7 Table

Table 1: Primers used to construct the *FpFCK1-GFP* reporter strain

Number	Name	Sequence
1	FCK1promF	CTGTAATACGACTCACTATAGGGAATATTAAGCTTTTGCGGCTTTAGCTAGGCTT
2	FCK1-gfpR	CACCATACCTCCGCCACCGACCCACTCAAGTTCACCCTTTCG
3	FCK1-gfpF	TGAACTTGAGTGGGTCGGTGGCGGAGGTATGGTGAGC
4	gfpR	TGGTCGGTCATTTCGAACCCCAGAGTCCCGCTTACTTGTACAGCTCGTC
5	HSV-tkF	GCGGGACTCTGGGGTTCGAAAT
6	HSV-tkF	CTTTTGGTTACGCCGTCAAGCTTTAACCTGAGGCTATG
7	gpdAF	CTCAGGTTAAAGCTTGACGGCGTAACCAAAAGTCAC
8	nptR	TCAGAAGAACTCGTCAAGAAGGC
9	FCK1termF	TTCTATCGCCTTCTTGACGAGTTCTTCTGAACTATAGCCATGAATAGAGTTCGAT
10	FCK1termR	GTGACATAACTAATTACATGATGCGGCCCTCTAGACGAGAGCGTCGTAGTCAGAC
11	CYC1R	GCGTGAATGTAAGCGTGAC
12	T7	TAATACGACTCACTATAGG

8 Figure legends

Figure 1: Read coverage analysis of *F. pseudograminearum FpFCK1-GFP* reporter strains. Four transformants (numbers 221, 223, 224 and 227) were whole genome sequenced and reads aligned to the predicted genome of a single copy insertion of the transforming DNA at the *FCK1* locus. The predicted locus is shown at the top of the image and the read coverage graphs below. The maximum read coverage depth observed in this region for any of the transformants was 55 reads and the y-axis has been set to this maximum for all four transformants. Transformants 221, 224 and 227 appear to have a single copy insertion based on the similar coverage of reads across the regions corresponding to the transforming DNA and the flanking DNA sequences not included in the vector used for transformation. Transformant 223 appears to have multiple insertions based on the higher read coverage of the transforming DNA.

Figure 2. FCK1-GFP induction in different nitrogen sources (A) and different pH (B). *FpFCK1-GFP* spores were grown in nitrogen source phenotyping plates (PM3) (A) and in pH phenotyping plates

(PM10) (B) for seven days. The colour scale from black to green indicates the range of the normalised GFP signals from weak to strong. The same colour scale was applied for the PM3 and PM10 plates.

Figure 3. FCK1-GFP induction in different nitrogen sources. *FpFCK1-GFP* spores were grown for seven days in minimal medium with arginine, asparagine, citrulline (**A**), citrulline with added glutamine or only glutamine as sole nitrogen sources (**B**). GFP signals were normalised to the culture optical density at 405 nm only if the OD_{405} was greater than 0.5 representing obvious fungal growth. These optical densities were typically reached 3 days post inoculation. The error bars show the standard error of the three technical replicates.

Figure 4. HPLC quantification of total fusatin (A) and DON (B) levels. *FpFCK1-GFP* and CS3096 spores were grown in minimal media with either asparagine, arginine, citrulline or citrulline with glutamine as sole nitrogen sources for seven days. Asterisks indicate statistical significance in a two-tailed student's t-test type two with * $p<0.05$ and *** $p<0.0005$.

Figure 5. Fluorescence microscopy of *FpFCK1-GFP* hyphae. *FpFCK1-GFP* spores were grown in minimal media with asparagine as sole nitrogen source for four days. The first column shows the GFP channel, the second a DIC image and the third an overlay. In the first row a hyphae can be seen and in the second row an ovoid cell. The scale bars indicate 10 µm.

Figure 6. Fluorescence microscopy of *FpFCK1-GFP* infected wheat seedlings. A and B show hyphae growing on the surface of intact seedlings 15 dpi and 11 dpi (last column). In C and D the coleoptile was removed to show hyphae growing in between the coleoptile and the pseudostem 10 dpi. E and F show hyphae growing in between the outer and inner leaf in an open cut pseudostem of a seedling 10dpi. A, C and E show bright field images and B, D and F GFP images.

Figure 7. Fluorescence microscopy of *FpFCK1-GFP* (A-D) and CS3096 (E, F) infected wheat seedlings. The wheat seedlings were imaged 15 days past inoculation. A and B show hyphae growing in between the first and second leaf, which have been pulled apart. In C and D the older first and second leaves have been removed to show hyphae growing on the youngest leaf (third) which was fully wrapped in the second leaf before. E and F show wheat seedlings infected with CS3096. A, C and E show bright field images and B, D and F GFP images.

Supplementary Figure 1. Disease assays with a Fusarium cytokinin producing strain of Fusarium graminearum. (A) Fusarium head blight assay with *F. graminearum* strain Ph1 and a transformant (Ph1+FpCK1) carrying the entire Fusarium cytokinin cluster. Assays were performed using susceptible Italian wheat cultivar A416. For Ph1 and Ph1+FpCK1 strains, 9 and 10 heads were

inoculated, respectively, with 10 µL of a 1×10^6 spores mL^{-1} suspension of macroconidia applied to a single central spikelet, covered with moistened plastic bags for 3 days and then scored 14 days post inoculation. Dashed lines are the mean and solid lines the median. No statistically significant differences were observed between the two strains in a t-test (p-value of 0.76). No symptoms were observed on water inoculated plants (not shown). Representative heads are shown. (B) An independent FHB assay using additional transformants (Ph1+FpCK34, Ph1+FpCK36 and Ph1+FpCK58) on susceptible wheat cultivar Apogee. Five biological replicates were used per strain with two central spikelets inoculated per head using 10 µL of a 1×10^5 spores mL^{-1} suspension of macroconidia. Symptoms were not observed on water inoculated control plants. Plants were scored 12 days post inoculation. An ANOVA detected no differences between strains (*p*-value = 0.108) although pairwise t-tests suggested Ph1+FpCK34 was slightly less virulent than Ph1 (*p*-value shown on graph). Representative heads are shown. (C) Fusarium seedling disease assay with Ph1, Ph1+FpCK1 and a mock control. Pre-germinated seedlings (4 days at room temperature) were inoculated on the central root with 250 µL of 5×10^5 spores mL^{-1} in macerated 0.9% agarose. Three biological reps were used with each replicate consisting of 10 plants that were pooled together prior to weighing shoot tissue. Values represented are the average weight of these three replicates divided by 10. Error bars represent the standard error of the mean. No statistically significant differences were observed between the two strains in a t-test (*p*-value 0.17).

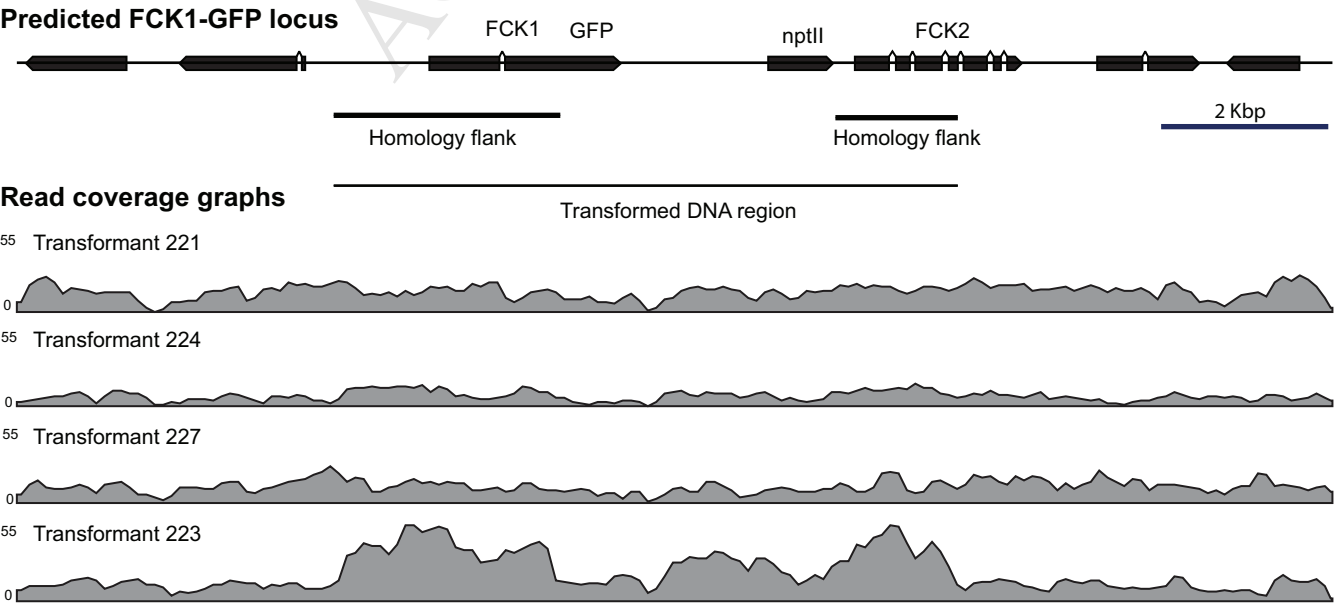

A

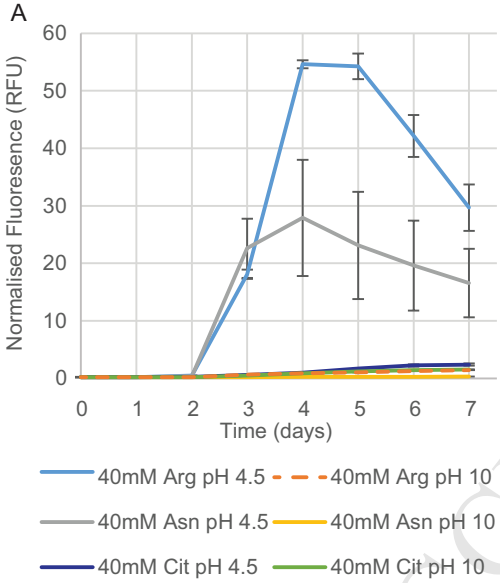

B

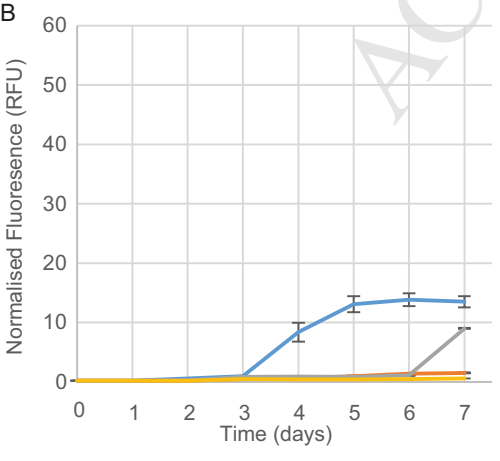

A

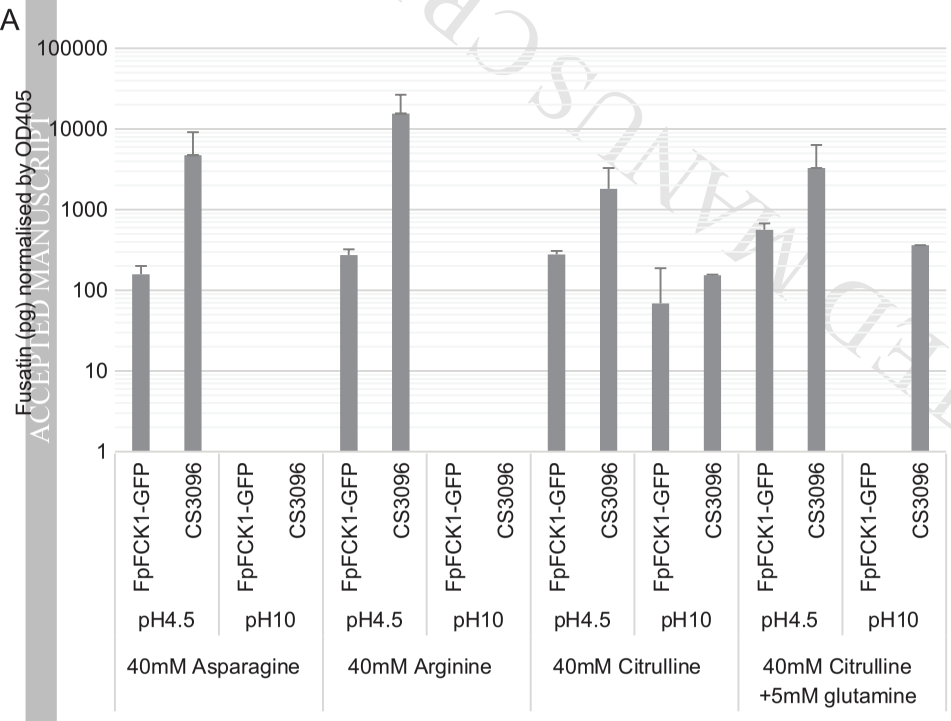

B